Noise Attenuation Technique Using the 2D Wavelet Transform and the Adaptive Deconvolution on Pre-Stack and Post-Stack data

Lucas José A. de Almeida*, CPGG/UFBA and Milton J. Porsani, CPGG/UFBA and INCT-GP/CNPq

Abstract

The wavelet transform uses wavelets in order to perform a spectral decomposition on seismic data, segregating it in several sub-bands. These sub-bands are oriented and contain somewhat precise frequency information, which depends on the wavelet that was used to apply the transform (Cohen, 1993). Since the ground roll is a type of seismic noise that is mostly vertically oriented, it will be separated from the rest of the non-vertical seismic events, making it easier to filter it without altering other seismic events of interest, such as the reflections. In this paper, the wavelet transform is used as a mean to segregate the ground roll from the reflections, while an adaptive deconvolution is applied only on the band where the ground roll is represented, in order to filter it. We applied the method using two different approaches: pre-stack and post-stack data. The results show that the post-stack application provided a better image.

Introduction

The ground roll is a dispersive linear noise, with low frequency, low velocity and high amplitude, that occurs frequently in land-based seismic acquisitions. This kind of noise tends to hide the reflections of the data, lowering the signal/noise ratio, making the velocity analysis more difficult and reducing the quality of the stacked section.

The wavelet Transform, as shown in (Miao and Cheadle, 1998) and (Matos and Osorio, 2002), can be used to decompose the seismic data into different oriented sub-bands, effectively segregating the ground roll from the signal of interest. While this decomposition is very effective in isolating the ground roll, one if it's weaknesses is that it can also drive shallow reflections to the vertical sub-band, causing the filtering process, whichever it might be, to also attenuate those reflections while striving to attenuate only the ground roll.

A method to solve this problem is to apply the wavelet transform on the post-stack data, on which, by the standard procedure, will be applied the normal moveout correction. By making the reflections horizontal, one can make them appear in any sub-band other than the vertical one, successfully preventing them from being attenuated. We show, via shot-gathers and stacked sections, that this solution is indeed effective for preserving shallow or low-velocity reflections when filtering the ground roll using the wavelet transform.

The Wavelet Transform

The wavelet transform (WT) uses compactly supported functions, denominated wavelets, in order to represent a given signal. By making the wavelet dilate or contract, the wavelet transform allows one to observe the signal at multiple resolution windows (Daubechies, 1992). This approach makes it more suitable to represent and analyze non-stationary signals, such as the seismic traces.

In it's discrete bi-dimensional form, the wavelet transform uses filter banks composed by a low-pass and a high-pass filter in order to decompose an image into various levels, according to the Multiresolution Analysis (Mallat, 1989). The decomposition procedure involves the convolution between the filter and the signal followed by a down-sampling operation, as shown in Figure 1. To obtain the reconstructed signal, it's sufficient to reverse the flow, using the appropriate filters.

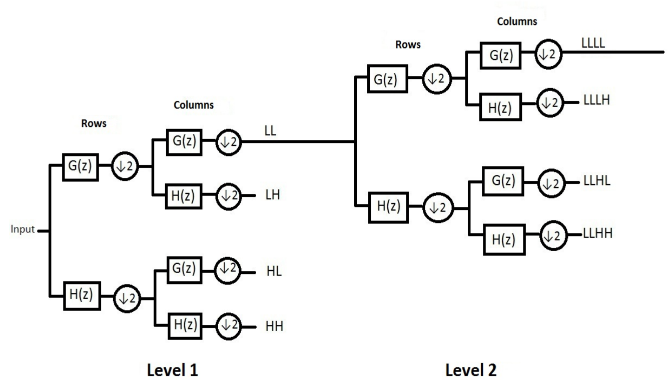

Figure 1: Discrete wavelet transform decomposition procedure. $G(z)$ and $H(z)$ represent the low-pass and high-pass filters, respectively.

Each level will contain four sub-bands, which will contain coefficients of different orientations and frequencies, depending on which dimension each filter was applied (Cohen, 1993). Figure 2 shows an schematic representation of the sub-bands in a three-level decomposition.

In the Figure above, the LH, HL and HH bands are denoted as the horizontal, vertical and diagonal sub-bands. Therefore, vertical events such as the ground roll, will appear in the vertical band (Matos and Osorio, 2002).

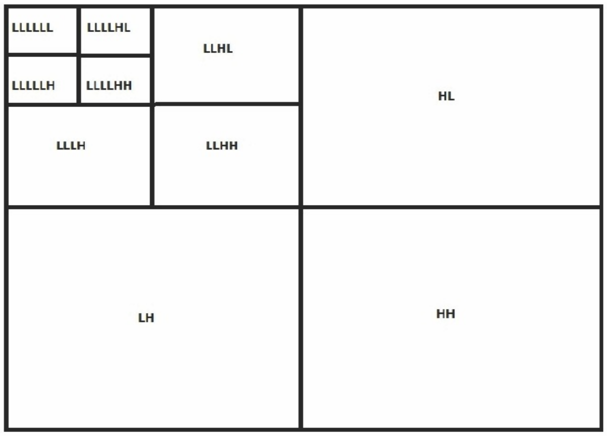

Figure 2: Sub-bands schematic representation in a three-level wavelet transform.

Therefore, the process used to filter the ground roll will be applied to the vertical sub-band.

Deconvolution

The deconvolution process is used, on land-based data, to improve vertical resolution by compressing the seismic pulse into an impulse. Because of it's effectiveness, this process is widely used by the oil and gas industry. However, in order to effectively use the process stated above, the seismic data has have a high signal to noise ratio or, so to speak, be almost free of noise (Yilmaz, 2001). In this paper, the deconvolution is used as temporal coherency filter, with the purpose of attenuating the ground roll after it's been separated from the other seismic events by the wavelet transform.

In this paper, the Morf algorithm is used in order to solve the prediction system (Morf et al., 1977). Along with that, we divide the initial seismic trace in several windows of l coefficients, in order to account for the fact that the seismic trace is not stationary. By using windows, we can assume that the portion of the seismic trace inside them is stationary, and we solve the system below and calculate a specific filter for each window, in a procedure denominated adaptive deconvolution.

For a filter containing two coefficients, the following system can be written (1), where x_m represent a seismic trace containing m samples and a_n, b_n represent the causal and anti-causal filters, respectively.

$$\begin{bmatrix} e_{a,3} & e_{b,1} \\ . & . \\ . & . \\ e_{a,t} & e_{b,t-2} \\ . & . \\ . & . \\ e_{a,l} & e_{b,l-2} \end{bmatrix} = \begin{bmatrix} x_3 & x_2 & x_1 \\ . & . & . \\ . & . & . \\ x_t & x_{t-1} & x_{t-2} \\ . & . & . \\ . & . & . \\ x_l & x_{l-1} & x_{l-2} \end{bmatrix} \begin{bmatrix} 1 & b_2 \\ a_1 & b_1 \\ a_2 & 1 \end{bmatrix} \qquad (1)$$

Solving the system above will yield two filters, a_n and b_n. For the purpose of filtering the ground roll, it was observed in (Almeida, 2013) that it's better to use a non-causal filter composed by the difference or sum of the above system's relative errors $e_{a,t}$ and $e_{b,t}$, and that the optimum value for the parameter n is 2. In this case, the filter used was composed by the difference between the relative errors, given by the equation (2), where $\tilde{b}_i = b_i/2$ e $\tilde{a}_i = a_i/2$.

$$h_t = \{-\tilde{b}_2, -\tilde{b}_1, 0, \tilde{a}_1, \tilde{a}_2\} \qquad (2)$$

Methodology

The filtering process was applied as follows:

- Decompose the data using the forward wavelet transform in as many levels as necessary;
- Use the deconvolution to filter only the vertical sub-band;
- Reconstruct the data using the inverse wavelet transform.

Results

The method was applied to the 50-RL-90 land-based seismic line, acquired in the Tacutu basin, Brazil. The line consists in 179 shots taken using a symmetric split-spread arrangement. The interval between receptors and shots was 50m and 200m, respectively; and the number of receptors used was 96. This generates a CDP coverage of 12.

Pre-Stack Filtering

The line went through the basic processing steps, such as geometry, mute and amplitude correction. In order to filter the ground roll, the wavelet transform was, then, applied using a three level decomposition scheme, followed by the adaptive deconvolution using the parameters $n = 2$ and $l = 20$; in the shot-gather domain. After that, the usual basic processing steps followed, such as velocity analysis, normal moveout correction and stacking.

As it can be seen in Figure 5 (a), the shot-gather is heavily affected by the ground roll. After the wavelet transform, the data is decomposed in it's various sub-bands. The vertical coefficients sub-band, which is the one filtered by the deconvolution, can be seen in Figure 4 (a). In Figure 5 (b), it's possible to see that the filtered data, while has efficiently attenuated the ground roll and preserved most of the seismic reflections, has it's shallow reflections attenuated. This is illustrated in Figure 7 (a), which represents the stacked section after the filtering proposed in Figure 5.

Post-Stack Filtering

In this case, the line went through the same processing steps listed in the previous section, minus the ground roll filtering in the shot-gather domain. Figure 6 (a) illustrates the stacked section without the noise filtering, which served as input for the wavelet decomposition in this stage. The filtering of the aforementioned stacked section using the method and parameters described in the previous section produced the result shown in Figure 7 (b). It can be seen that the reflections, in this result, are well preserved; specially the shallow ones. Figure 7 shows a detail from both stacked sections, in which can be seen the superiority of the post-stack approach.

Conclusions

The ground roll filtering using the wavelet transform can be applied either to pre-stack or post-stack data. In this paper, we compared both approaches. While the pre-stack filtering approach resulted in a shot-gather with less noise and preserved seismic reflections, it's shallow reflections were greatly attenuated. The post-stack filtering did better in this point, as it effectively attenuated the ground roll while also preserving the shallow seismic reflections. In conclusion, both approaches are valid, although the post-stack one was clearly better.

It's important to observe that the post-stack approach does not depend on any stages prior to it's application, and post-stack methods such as the post-stack deconvolution could be applied after it in order to refine the final stacked section. If relevant pre-stack procedures which depend on the noise attenuation are to be applied, one can obtain a result similar to the post-stack approach by applying the normal moveout correction and then reorganize the data into shot-gathers, as shown in (Almeida, 2013).

References

Almeida, L. J. A., 2013, Atenuação do *Ground Roll* Utilizando a Transformada Wavelet em Conjunto com a Deconvolução Adaptativa, Trabalho de Graduação, Universidade Federal da Bahia.

Cohen, J. K. and Chen, T., 1993, Quantitative dip bounds for the two-dimensional discrete wavelet transform, Mathematical Methods in Geophysical Imaging, 140.

Cheadle, S. and Miao. X, 1998, Noise attenuation with wavelet transforms, SEG Annual Meeting, pp. 1072-1075.

Daubechies, I., 1992, Ten lectures on wavelets, SIAM CBMS-NSF Regional Conference Series in Applied Mathematics.

Mallat, S., 1989, A theory for multiresolution signal decomposition: The wavelet representation, Trans. on Pattern Analysis and Machine Intelligence, IEEE, 7:674693.

Matos, M. C. and Osorio, P. L. M., 2002, Wavelet transform filtering in the 1d and 2d for ground roll suppression, SEG Annual Meeting, pp. 2245-2248.

Morf, M.; Dickinson, B.; Kailath, T.; and Vieira, A., 1977, Efficient solution of covariance equations for linear prediction, Trans. on Acoustics, Speech and Signal Processing, IEEE, 25:429-433.

Yilmaz, O., 2001, Seismic data analysis: processing, inversion and interpretation of seismic data, SEG.

Acknowledgements

The authors wish to express their gratitude to CAPES, INCT-GP/CNPq/MCT, PETROBRAS, ANP, FINEP, FAPESB Brazil for financial support. We also thank LANDMARK for the licenses granted to CPGG/IGEO/UFBA.

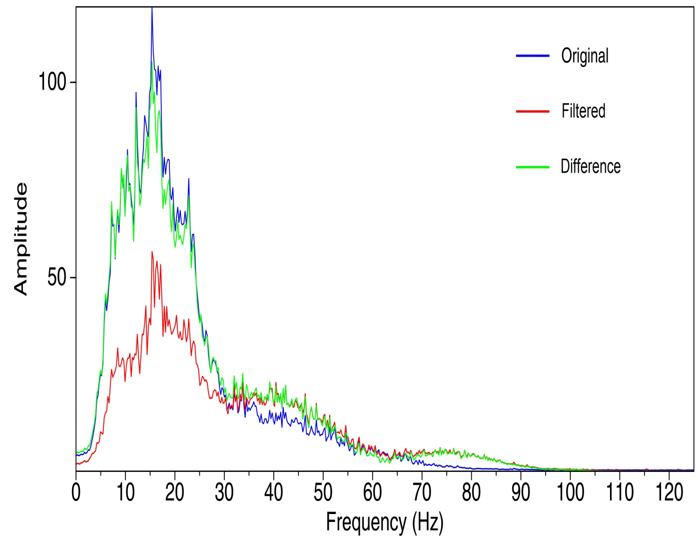

Figure 3: Frequency spectrum for the shot-gathers of Figure 4.

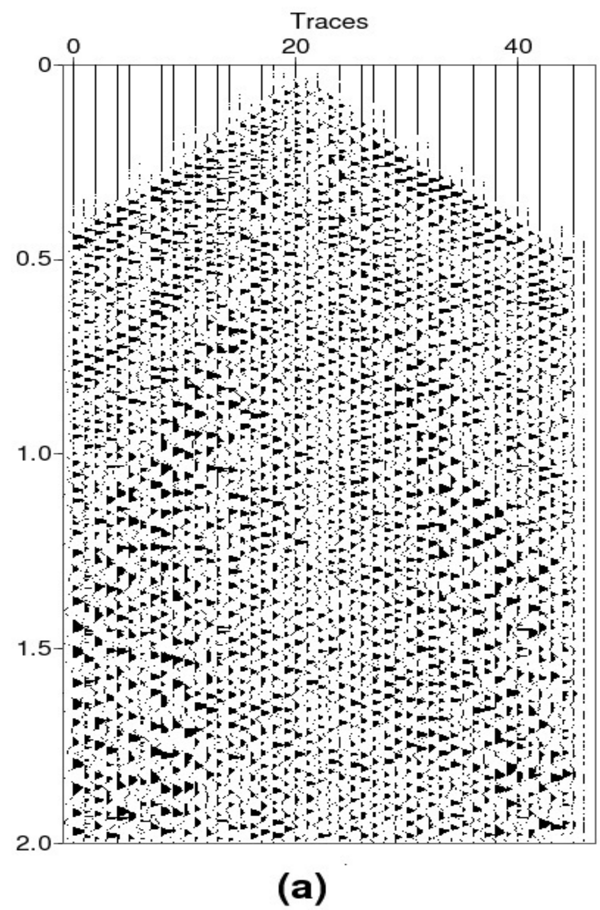

Figure 4: (a) - Vertical sub-band of the first level of the wavelet decomposition for the shot-gather present on Figure 5 (a).

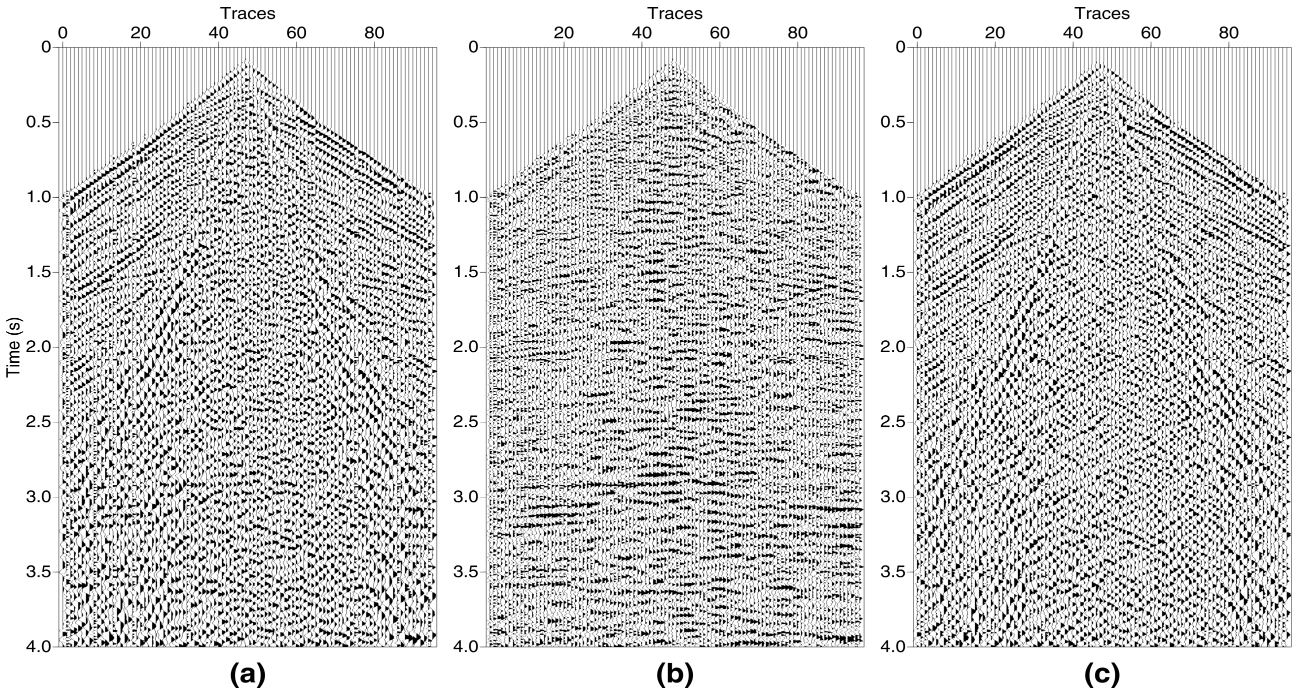

Figure 5: Shot-gathers. (a) - Original. (b) - After filtering using the wavelet transform and the deconvolution. (c) - Difference between (a) and (b).

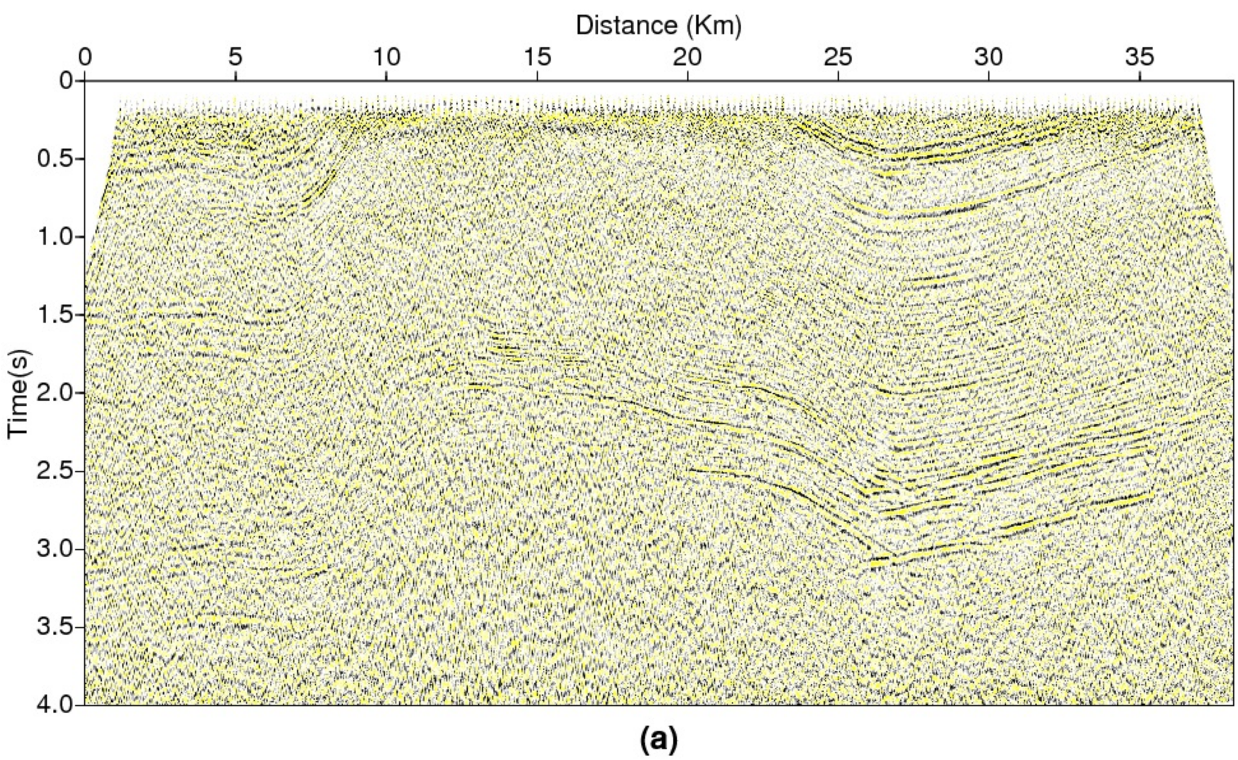

Figure 6: (a) - Original stacked section.

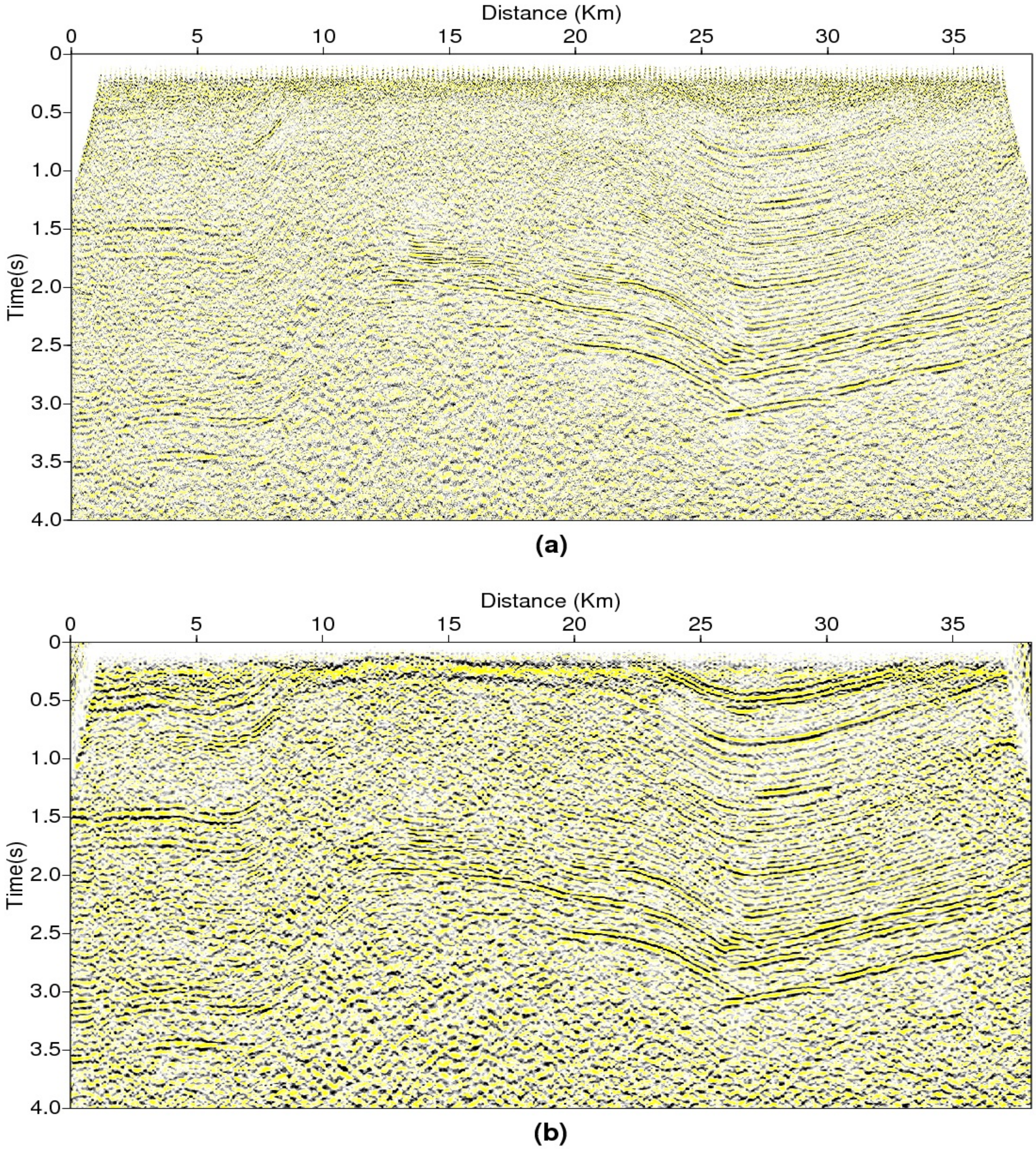

Figure 7: (a) - Stacked section filtered using the wavelet decomposition and deconvolution pre-stack. Correspondent shot-gather is shown in figure 7. (b) - Stacked section after filtering using the wavelet decomposition and deconvolution on the post-stack data show in Figure 5 (a).

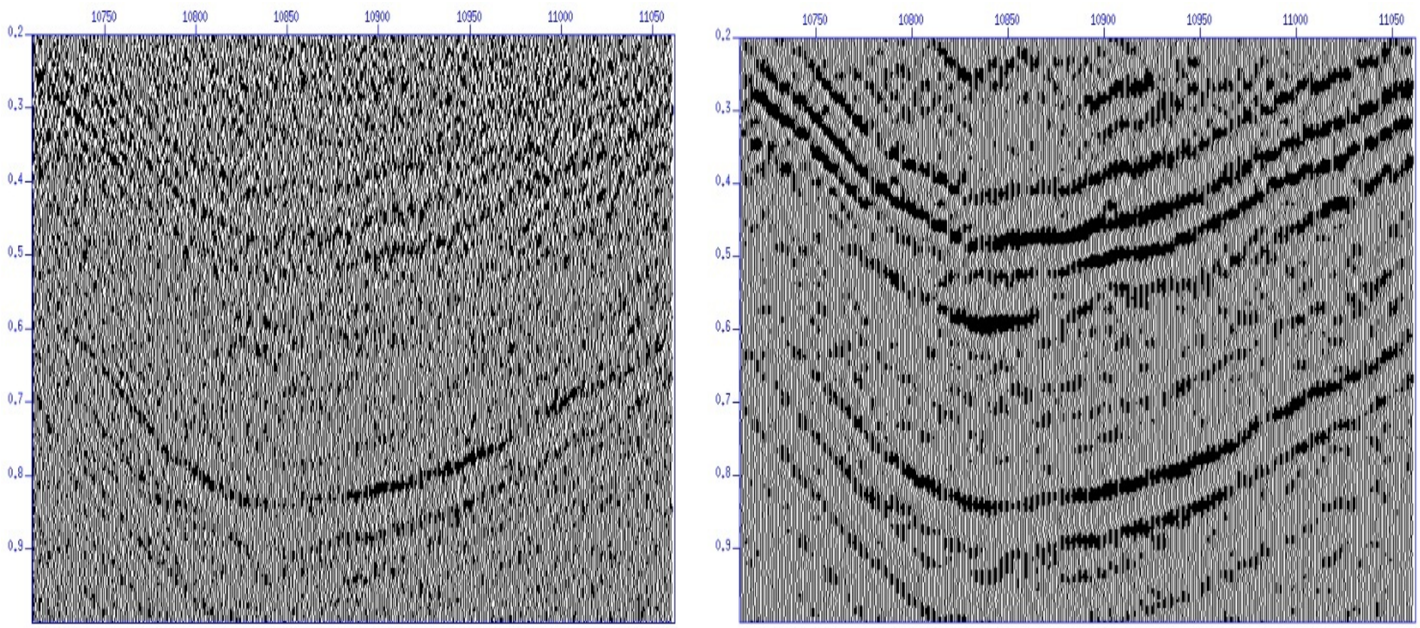

(a) (b)

Figure 8: Detail from: (a) - Figure 6 (a). (b) - Figure 6 (b).